Published in final edited form as:
Anal Chem. 2008 December 1; 80(23): 8975–8981.

High-Throughput Quantitative PCR in Picoliter Droplets

Margaret Macris Kiss[1], **Lori Ortoleva-Donnelly**[1], **N. Reginald Beer**[2], **Jason Warner**[1], **Christopher G. Bailey**[2], **Bill W. Colston**[2], **Jonathon M. Rothberg**[1], **Darren R. Link**[1,*], and **John H. Leamon**[1]

[1] Raindance Technologies, 44 Hartwell Ave., Lexington, MA 02421

[2] Lawrence Livermore National Laboratory, 7000 East Ave., Livermore, CA 94551

Abstract

Limiting dilution PCR has become an increasingly useful technique for the detection and quantification of rare species in a population, but the limit of detection and accuracy of quantification are largely determined by the number of reactions that can be analyzed. Increased throughput may be achieved by reducing the reaction volume and increasing processivity. We have designed a high-throughput microfluidic chip that encapsulates PCR reagents in millions of picoliter droplets in a continuous oil flow. The oil stream conducts the droplets through alternating denaturation and annealing zones, resulting in rapid (55 second cycles) and efficient PCR amplification. Inclusion of fluorescent probes in the PCR reaction mix permits the amplification process to be monitored within individual droplets at specific locations within the microfluidic chip. We show that amplification of a 245 bp Adenovirus product can be detected and quantified in 35 minutes at starting template concentrations as low as one template molecule per 167 droplets (0.003 pg/μL). The frequencies of positive reactions over a range of template concentrations agree closely with the frequencies predicted by Poisson statistics, demonstrating both the accuracy and sensitivity of this platform for limiting dilution and digital PCR applications.

INTRODUCTION

The ability to quantify a small number of targets against a background of highly homologous targets is central to applications ranging from environmental monitoring to clinical diagnostics. PCR is the most sensitive method for identification of rare species in a complex sample, but the DNA derived from the more abundant species provides a vast excess of sequences that can compete with rare sequences for the PCR primers.[1] Therefore, it is difficult to quantify the fraction of poorly represented targets in a starting population when amplification is carried out in bulk reactions.[1,2]

Limiting dilution PCR has become an increasingly useful technique for determining the total number of initial DNA targets present in a complex mixture, such as cells isolated from a tumor or a diverse microbial community.[1–3] Using the limiting dilution PCR strategy, accurate quantitation of targets can be achieved by serially diluting the sample and performing multiple reaction replicates to the point that individual reactions contain single template molecules.[1] A qualitative “all or none” end point signal is used to score the positive and negative reactions, and the number of targets present in the initial reaction can then be quantified from the proportion of positive reactions using Poisson statistics.[1] Since individual template molecules can be separated and amplified independently using limiting dilution PCR, amplification bias

*To whom correspondence should be addressed: Dr. Darren Link, Raindance Technologies, 44 Hartwell Ave., Lexington, MA 02421. E-mail: dlink@raindancetechnologies.com Phone: (781) 861-6300, Fax: (781) 861-1233.

is avoided, and products exclusively derived from a single template are generated. The limiting dilution technique has been used to enumerate unculturable organisms in the environment[3] as well as to detect rare mutations associated with colorectal cancer via "digital PCR," in which fluorescent probes that discriminate the product material provide a digital readout of the fraction of a mutant sequence in the population.[2]

Rigorous statistical analysis is required to establish significance using the limiting dilution PCR technique, since positive signals should be distributed according to Poisson probabilities.[1,2] According to Poisson statistics, many empty reactions are required in order to maximize the number of reactions containing only single-copy targets. Therefore, the limit of detection of rare species is largely determined by the number of reactions that can be analyzed.[2] Consequently, the utility of limiting dilution PCR techniques is severely limited by the low number of reactions that can be performed by conventional PCR cyclers (thousands of reactions/day) and the prohibitive costs associated with the large volumes of reagents (typically > 0.1 μL/well) and large numbers of microwell plates required to perform millions of reactions.

Microfluidic systems for PCR offer the advantages of reduced reaction volumes, higher thermal cycling speed, and decreased reagent and sample consumption, which is critical when limited template material is available from clinical or environmental samples. The majority of such systems utilize fabricated micro-, nano-, or picoliter reservoirs for conventional thermocycling[4–7] or a continuous-flow based approach in which the temperature is kept constant over time at specific locations in the system, and the sample is moved between the individual temperature zones for cycling.[8,9] Substantial increases in throughput and reduced (picoliter) reaction volumes can be achieved by emulsion PCR, in which reactions are conducted in water-in-oil emulsions. This method was first used to amplify single DNA molecules [10] and is now used commercially to generate clonally amplified templates from complex libraries of DNA fragments to facilitate next-generation sequencing.[11] The emulsification technique is well suited to digital PCR applications, as each amplicon is isolated in its own droplet preventing amplification biases due to the preferential amplification of one template over another.[12–14] Current methods of bulk emulsification, however, generate droplets that are non-uniform in size,[11] and real-time analysis of individual reactions, which is critical to the digital PCR concept, cannot be accomplished.

Alternatively, microfluidic systems can be designed to generate monodisperse droplets in a microchannel through shearing flow at a T-junction or a flow-focusing zone.[15–18] Microfluidic systems offer increased control over droplet size, and amplification of single DNA molecules in droplets generated by microfluidic devices has recently been demonstrated.[19,20] If the droplet generation architecture is implemented on a PCR chip, individual droplets can be focused in the channel for optical interrogation during amplification.[20–22] Here, we describe a continuous-flow-based real-time PCR system that generates discrete, picoliter-scale PCR reactions in a continuous stream of inert fluorinated oil. The PCR reaction droplets are conveyed by the oil flow through channels in a microfluidic chip. Static thermal zones controlled by heaters below the chip provide 35 cycles of two-step PCR. Periodic channel constrictions or "neckdowns" permit a fluorescence signal to be measured in real time from each individual droplet, providing information on amplification efficiency within each droplet. This system provides high-throughput, low-labor DNA amplification of millions of reactions per hour combined with real-time monitoring of individual reactions. We show that amplification of a 245 bp Adenovirus product can be detected in 35 minutes at starting template concentrations as low as one template molecule per 167 droplets (0.003 pg/μL). The frequencies of positive reactions over a range of template concentrations agree closely with the frequencies predicted by Poisson statistics, demonstrating both the accuracy and sensitivity of this platform for limiting dilution and digital PCR applications. We discuss how this system provides simple yet effective solutions to the challenges of sample collection, contamination,

and processing, and generates discrete, clonally amplified products amenable to multiple research needs.

EXPERIMENTAL SECTION

Chip Preparation

Fluidic chips were fabricated using soft lithography.[23] The masters for these chips were produced by coating 4-inch silicon wafers with SU8 photoresist (MicroChem. Corp., Newton, MA) and exposing the desired pattern through a mask with UV light on an OAI Hybralign Series 200 Mask Aligner (OAI, San Jose, CA). Multilevel structures were created by repeating the above processing with layers of desired varying thickness. The droplet generation and neckdown regions of the chip were 50 microns deep while the incubation channels on the master had a depth of 260 microns. The body of the chip was formed by PDMS-based replica molding [24], and the resulting 70 mm × 75 mm slab was cut from the mold, placed in an oxygen plasma to activate the surface, and irreversibly bonded [25] to a 70 mm × 75 mm glass microscope slide.

PCR Amplification

Experiments were conducted using a PCR primer and probe set designed for the Adenovirus genome (pAdeasy-1 vector, Stratagene, La Jolla, CA) (See Table 1). The PCR master mix contained 50 mM Tris/HCl (pH 8.3), 10 mM KCl, 5 mM $(NH_4)_2SO_4$, 3.5 mM $MgCl_2$, 0.2 mM dNTP (Invitrogen, Carlsbad, CA), 0.5% Tetronics (Research Diagnostics Inc., Flanders, NJ), 0.1 mg/ml BSA (Sigma-Aldrich, St. Louis, MO), 0.2 units per μL of FastStart Taq DNA polymerase (Roche Applied Sciences, Indianapolis, IN), 0.5 μM each of forward and reverse primers (Integrated DNA Technologies, Coralville, IA), 0.25 μM FAM-labeled probe quenched with a 3′ BHQ1 (Biosearch Technologies, Novato CA), and 1 μM Alexa Fluor 594 (Invitrogen, Carlsbad, CA).

Serial dilutions of the pAdeasy vector were made from a 5 nM (100 ng per μl) stock solution to concentrations ranging from 60 to 0.0006 ng per μl. Concentrations were verified by traditional qPCR using a Chromo4 real-time PCR machine (Bio-Rad, Hercules, CA), with a 3-minute hot start at 95°C followed by 40 cycles at 95°C for 10 seconds, 65°C for 30 seconds, and 68°C for 30 seconds with plate reads after the 65°C and 68°C steps at each cycle. Target concentrations for the serial dilutions were chosen to reflect specific numbers of template molecules per 65 picoliter volume, the volume of droplets generated by the fluidic chip (See Table 2). Seven 200 μl reaction mixes were generated, one for each of the target dilutions listed in Table 2, spanning template concentrations from 0.006 to 600 template molecules per 65 pL.

The mixture of template and PCR reagents was delivered to the chip at a rate of 125 μL/h from a 1 mL glass syringe controlled by a custom Harvard Syringe Pump (Harvard Apparatus, Holliston, MA). The syringe was connected to 1/16-inch PEEK tubing, (length less than the 3m shown to interfere with qPCR),[26] that had been passivated by flowing a mixture containing 5 mg/ml tRNA (Sigma-Aldrich, St. Louis, MO) in Tris-EDTA buffer to minimize DNA loss in low concentration samples through adsorption to the tube walls. The oil/surfactant mix (GEA, RainDance Technologies, Lexington, MA) was contained in a 5 ml glass syringe and delivered to the chip at a rate of 500 μL/h. Reactions were infused through the chip sequentially from lowest to highest concentration, the chip was completely flushed with oil following amplification, and the syringes and PEEK tubing were replaced between samples.

Reaction droplets were formed via flow-focusing [27] whereby a perpendicular intersection between the channel through which the PCR reaction mix was infused and two channels flowing immiscible oil resulted in the generation of uniform, monodisperse droplets of approximately 65 picoliters (50 μm diameter) (Fig. 1b). The chip was mounted on two 24 volt,

30 watt silicon heating elements (Watlow, St. Louis, MO) that divided it into two thermal zones, a 95°C zone and a 67°C zone (Fig. 1a). The droplets were conveyed through the chip by the flow of oil, and the static thermal zones provided hot start activation followed by 34 cycles of two-step PCR. The velocity at which the droplets moved through the chip was controlled by regulating the injection rate of the oil and PCR mix and could be further reduced by extracting interstitial oil from around the PCR droplets (Fig. 1a), thereby increasing the droplet packing and decreasing the flow rate through the channels. Using these two methods of velocity control, droplets experienced a 3-minute, 95°C hot start, followed by 34 cycles of a 15 second denaturation phase (95°C) and a 40 second annealing/extension phase (67°C). Cycles 5, 6, and 7 had slightly shorter annealing/extension times (Fig. 1a).

As any given sample was amplified on the microfluidic chip, the emulsion was collected from the exhaust line in a 1.5ml microcentrifuge tube throughout the duration of the reaction. Once the sample had been completely processed through the chip, the emulsified drops were broken by flash-freezing in liquid nitrogen for 10 seconds and subsequently centrifuged at 16,000 g for 10 minutes in a benchtop mini-centrifuge. The upper, aqueous layer was removed and analyzed both by gel electrophoresis on a 2% agarose TAE gel and simultaneously on the Agilent 2100 Bioanalyzer (Agilent Technologies, Santa Clara, CA) to confirm the size and quantity of the products.

Data Acquisition and Analysis

Droplets were interrogated at specific “neckdowns”, 100 micron long regions of the chip where the channel width and depth decreased forcing droplets into a single file. The neckdowns were spaced periodically throughout the chip, providing fluorescence data at the time of droplet generation as well as during the annealing and extension phase at cycles 4, 8, 11, 14, 17, 20, 23, 26, 29, 32, and 34. The fluorescent signal at both 530 and 650 nm wavelengths was monitored at each of the 12 observation points on the chip (the nozzle and the 11 cycle locations). A 561 nm laser (Coherent, Inc., Santa Clara, CA 300 mW) was used to excite Alexa Fluor 594, which emitted at 650 nm and served as an internal control for droplet detection. A 488 nm laser (Coherent, Inc., Santa Clara, CA 150 mW) excited the FAM fluor, which when released from its proximity to the Black Hole quencher on the Taqman probe by polymerase exonuclease activity, emitted at 530 nm. Fluorescence was recorded using a custom optics system consisting of a 20X objective lens (Carl Zeiss MicroImaging, Thornwood, NY) and two filters (530/40 nm and 650/40 nm) (Edmund Optics, Barrington, NJ) fitted to 300–650nm, 0.1V/μA Photo-Multiplier Tubes (Hamamatsu, Bridgewater, NJ). Signals from the PMTs were passed to a Dell Optiplex GX620 computer via a custom data acquisition board. Data was acquired at a rate of 222,222 Hz, down-sampled 3-fold to approximately 74,000 reads per second, and stored for subsequent analysis. The 1.5V, 100 mA 850 nm LED (OSRAM Opto Semiconductors, Inc., Santa Clara, CA) provided non-conflicting strobe illumination that permitted acquisition of visual images with a Guppy CCD camera (Allied Vision Technologies, Newburyport, MA).

Fluorescence data from each neckdown on the chip was analyzed with custom software written in Labview (National Instruments Corp., Austin, TX). Alexa Fluor 594 fluorescence values above background were used to identify drops, and the FAM fluorescence, indicative of relative DNA concentration, was recorded for each. Baseline levels of FAM fluorescence were obtained from the median value of the FAM fluorescence recorded from droplets in neckdowns 0 through 11. PCR positive drops, or drops in which PCR amplification had occurred, were identified as drops with a FAM signal greater than two standard deviations over the median baseline signal.[28] The percentage and fluorescent signal of PCR positive drops were recorded at each neckdown for every sample. Cycle thresholds were calculated from a plot of average droplet fluorescence versus cycle number where curves were in the exponential phase. The MPN (most

probable number) calculation was made from the data (percentage of PCR positive droplets) obtained at the 4 lowest dilutions of template DNA.[29]

RESULTS AND DISCUSSION

To address the need for high-throughput, real-time PCR, we have designed a disposable PDMS/glass microfluidic chip that can be used to carry out continuous-flow droplet-based PCR reactions (Fig. 1a). To generate droplets, a syringe pump was used to infuse the aqueous sample into a channel on the chip. This channel perpendicularly intersected two channels flowing immiscible oil, resulting in the generation of droplets with a narrow size distribution.[27] Figure 1b shows the generation of droplets at the chip nozzle. The 65 picoliter droplets had an average diameter of 50 μm and were generated at a rate of 500 per second or 1.8 million per hour.

To carry out PCR, the chip was mounted on two static heaters that divided it into two thermal zones, a 95°C zone and a 67°C zone. The droplets were conveyed through the chip by the flow of oil, and the static thermal zones provided hot start activation and 34 cycles of two-step PCR (Fig. 1a). Downstream of the nozzle, the channel depth expanded from 50 μm to 260 μm, decreasing the droplet separation and increasing the droplet density (Fig. 1c). The velocity at which the droplets moved through the chip was controlled by regulating the infusion rate of the oil and PCR mix and could be further reduced by extracting interstitial oil from around the PCR droplets (Fig. 1a), thereby increasing the droplet packing and decreasing the flow rate through the channels. Using these two methods of velocity control, droplets experienced a 3-minute hot start activation followed by 34 cycles (95°C for 15 seconds, 68°C for 40 seconds with slightly shorter cycle times for cycles 5, 6, and 7 as shown in Fig. 1a) resulting in a total reaction time of approximately 35 minutes. The variation of transit time through the delay line is estimated to be less than 5% due to a tendency for the droplets to move together through the device. These cycling times were not optimized, and amplification of the relatively short 245 bp product could likely be achieved with shorter cycles. This would improve the system throughput by allowing the rates of infusion of oil and PCR mix, and accordingly, the rate of droplet generation at the nozzle to be increased.

To assess the utility of the system for quantitative PCR applications, serial dilutions of the Adenovirus genome were made at 600, 60, and 6 template molecules per 65 picoliter droplet, as well as at one template molecule per 2, 3, 17, and 167 droplets (0.6, 0.3, 0.06, and 0.006 copies per droplet, respectively). The concentrations of the diluted DNA were verified by qPCR using a traditional real-time thermocycler. The reactions were infused through the chip sequentially from lowest to highest concentration, the chip was completely flushed with oil following amplification, and the syringes and PEEK tubing were replaced between samples to prevent contamination that could lead to the appearance of false positives. While the chips are disposable, they were not replaced between runs when proceeding from a low to high concentration of the same template.

The PCR microchip was stationed above an optical system that combined a video camera with a two wavelength laser excitation and detection system. Using this optical system, droplets were interrogated at specific “neckdowns”, 100 micron long regions of the chip where the channel width and depth decreased forcing droplets into a single file (Fig. 1c). Since the diameter of the droplets was the same as the width and depth of the neckdowns, only a single droplet could fit through a neckdown at one time, and no droplets could be missed by the lasers. The neckdowns were spaced periodically throughout the chip, providing fluorescence data at the time of droplet generation as well as during the annealing and extension phase at cycles 4, 8, 11, 14, 17, 20, 23, 26, 29, 32, and 34. A fluorescent dye, Alexa Fluor 594, provided a constant signal in each droplet that was used for droplet detection without inhibiting PCR amplification efficiency or yield (data not shown). This signal (average value of 1.5 ± 0.2 fluorescence units)

and the peak width at half the maximum signal (average value of 156 ± 13 μs) did not fluctuate significantly, indicating that the droplet size was uniform. In addition to the Alexa dye, a FAM-labeled Taqman probe specific to a region of the amplified Adenovirus sequence was added to the reaction mix (Table 1). Fluorescence of the FAM dye on the probe could be detected under the FRET (fluorescence resonance energy transfer) process when released from its proximity to a quencher by the exonuclease activity of the DNA polymerase, providing a fluorescence intensity increase proportional to DNA concentration in the droplet.[30] As the emission wavelengths for the Alexa and FAM dyes did not overlap, the two dyes could be interrogated without cross-talk, permitting accurate, simultaneous detection of both droplet number and DNA content.

Data from the on-chip PCR reactions is presented in Figure 2. Approximately 30 seconds of data was collected at each neckdown, resulting in the analysis of an average of 14,000 ± 2700 drops per cycle. As individual droplets passed through the excitation lasers (488 nm and 561 nm) at the interrogation neckdowns, both the Alexa Fluor 594 and FAM signals were recorded. The observed fluorescence signals at the final neckdown (cycle 34) are plotted versus the number of droplets in Figure 2a. The distribution of Alexa Fluor 594 signal was narrow for droplets analyzed at all of the template concentrations. In contrast, a bimodal distribution of FAM fluorescence was observed for droplets with starting template concentrations of less than one molecule per droplet (Fig. 2a, panels I–IV), indicating the presence of two populations. These populations correspond to empty droplets and droplets that supported amplification. At the lowest template dilution (Fig. 2a, panel I), the second FAM peak corresponding to PCR-positive droplets was small, indicating that amplification had occurred in very few of the droplets. The size of the population with higher FAM fluorescence increased as the number of droplets containing template was increased (Fig. 2a, panel II–V). At a starting template concentration of 60 copies per droplet, amplification was detected in almost all of the droplets, and a single population of droplets with high FAM fluorescence was observed (Fig. 2a, panel VI).

The empty droplets and PCR-positive droplets are further distinguished in Figure 2b which shows a time trace of fluorescence signals from droplets as they passed one-by-one through the excitation lasers at the final interrogation neckdown. The Taqman probe provided a background FAM fluorescence in all droplets (average value of 2.3 ± 0.1 fluorescence units), but the FAM signal was increased by approximately 1.2 fluorescence units in droplets in which amplification had occurred (average value of 3.5 ± 0.2 fluorescence units). No statistical difference was observed (p-value =0.37) between the Alexa 594 signals recorded from droplets exhibiting a positive Taqman signal and those that were PCR negative (Fig. 2b), indicating that the PCR signal was independent of the Alexa Fluor signal.

For each of the Adenovirus dilutions examined, the percentage of PCR positive droplets was plotted versus cycle number (Fig. 2c). Successful amplification was detected at Adenovirus concentrations as low as one template molecule per 167 droplets (0.006 copies per drop). As expected, the percentage of droplets that supported amplification increased as the starting template copy number per drop was increased (Fig. 2a, c). Following amplification, the droplets collected from the chip were broken and analyzed by automated electrophoresis to confirm a product of the appropriate size (Fig. 3). Consistent with the fluorescence data, the gel showed an increase in total product as the amount of starting material was increased.

The timing of appearance of PCR positive droplets was delayed as the concentration of starting material was reduced (Fig. 2c). Accordingly, cycle thresholds calculated from curves of average droplet fluorescence versus cycle number for starting template concentrations of greater than 1 copy per droplet showed an approximately 2 to 3 cycle shift in cycle threshold when the template concentration was increased by an order of magnitude (Table 2). A plot of

the log of concentration versus cycle threshold showed a slope consistent with an amplification efficiency of 2.4 (data not shown). This represents a 20% increase over the expected value and suggests a need for optimization of the design to enhance the utility of the system for qPCR applications in high titer regions (>3pg/μL), which could perhaps be achieved by adding more interrogation neckdowns.

To determine the accuracy of the system for quantifying low concentrations of starting material, the observed titers were compared with the average percentage of positive reactions predicted for each starting template concentration by Poisson statistics and by MPN (most probable number) (Table 3). Poisson statistics in real-time, single-copy picoliter droplet PCR and RT-PCR was previously demonstrated, but the total droplet count was limited by the architecture,[19,31] which allowed analysis of a maximum of 1000 droplets using a static system. Due to the continuous flow nature of the system described here, the amplification and imaging of over a million droplets was possible in a 35-minute run, thereby overcoming the droplet count limitation. Figure 4 shows a plot of the percentage of droplets that supported amplification versus starting copy number compared to that predicted by Poisson (solid blue line). Very good agreement was seen, but a small shift in slope and offset may be indicative of some sample loss through adsorption to the tube walls. Interestingly, at the lowest template dilutions (0.006 and 0.06 copies per droplet), the PCR positive droplets were slightly overrepresented (11.7% observed versus 5.8% expected at 0.06 copies per droplet). This observation could be indicative of a limitation in the accuracy of serial dilutions in this range or of some false positive in the algorithm for distinguishing amplified and unamplified droplets. It is also possible that there was some low level of template contamination during preparation of the samples.

To estimate the actual starting concentration of template in the reactions, the MPN (most probable number) technique that is commonly used to estimate microbial population sizes[32] was employed. The MPN technique relies on the pattern of positive and negative reactions across several serial dilution steps to derive a population estimate based on the mathematics of Halvorson and Ziegler.[33] Using this methodology, an MPN of 0.83 template molecules was calculated for a 1 copy per droplet dilution. This calculation was based on the 4 lowest dilutions of starting material, although the MPN could be as high as 1.1 copies if data from only the 3 lowest dilutions of template DNA was used.[29] Table 3 shows the corrected template copy numbers per droplet based on the MPN calculation. The Poisson expected PCR positive droplets determined by the adjusted starting template concentrations were compared with the observed values (Table 3). Even closer agreement was evident at starting template concentrations of 0.3 (20.3% observed versus 21.6–22.4% expected), 0.6 (32.5% observed versus 38.6–39.8% expected), and 6 copies per droplet (89.0% observed versus 99.2–99.3% expected). Given the accuracy of the data for endpoint analysis this droplet-based strategy appears to be ideal for quantitative PCR applications that require single molecule detection.

CONCLUSION

We have shown that on-chip PCR in picoliter droplets provides a solution to the limitations of throughput and cost associated with limiting dilution PCR techniques that require millions of reactions to detect single-copy target nucleic acids from a complex environment. By partitioning microliter scale samples into discrete, picoliter droplets, this system increases the number of reactions that can be performed from thousands of reactions per day to millions per hour, offers great advantages in terms of reagent savings, and reduces time-costly manual preparation steps that increase the risk of sample contamination. In addition to providing high-throughput PCR, this platform generates droplets that are uniform in diameter, allowing for constant reaction rates across the droplets and highly reproducible amplification, which is difficult to achieve with bulk emulsions that have distributions in droplet diameter of up to two orders of magnitude. In addition, the use of a microchip with periodic channel restrictions, or

neckdowns, allows detection of individual droplet fluorescence in real time, which is not feasible with bulk emulsion PCR. This proof of principle study demonstrates high sensitivity (detection of template concentrations as low as 0.003 pg/μL in 35 minutes) combined with reliable quantification of targets (close agreement with Poisson statistics over a range of template concentrations) using the current design. These results show the great promise of this technology for limiting dilution qPCR applications. Future efforts will focus on multiplex library amplification, droplet merging,[34] sorting of "empty" droplets,[34] and including bead-bound primers or templates within the droplets.[11,19]

Acknowledgments

This work was supported by the NIH (NCI 1R21 CA125693-01). The contribution of authors N.R. Beer, C.G. Bailey, and B.W. Colston was performed under the auspices of the U.S. Department of Energy by Lawrence Livermore National Laboratory under Contract DE-AC52-07NA27344. The project #06-ERD-064 was funded by the Laboratory Directed Research and Development Program at LLNL.

References

1. Sykes PJ, Neoh SH, Brisco MJ, Hughes E, Condon J, Morley AA. Biotechniques 1992;13:444–449. [PubMed: 1389177]
2. Vogelstein B, Kinzler KW. Proc Natl Acad Sci U S A 1999;96:9236–9241. [PubMed: 10430926]
3. Ottesen EA, Hong JW, Quake SR, Leadbetter JR. Science 2006;314:1464–1467. [PubMed: 17138901]
4. Marcus JS, Anderson WF, Quake SR. Anal Chem 2006;78:956–958. [PubMed: 16448074]
5. Matsubara Y, Kerman K, Kobayashi M, Yamamura S, Morita Y, Tamiya E. Biosens Bioelectron 2005;20:1482–1490. [PubMed: 15626601]
6. Morrison T, Hurley J, Garcia J, Yoder K, Katz A, Roberts D, Cho J, Kanigan T, Ilyin SE, Horowitz D, Dixon JM, Brenan CJ. Nucleic Acids Res 2006;34:e123. [PubMed: 17000636]
7. Nagai H, Murakami Y, Morita Y, Yokoyama K, Tamiya E. Anal Chem 2001;73:1043–1047. [PubMed: 11289415]
8. Liu J, Enzelberger M, Quake S. Electrophoresis 2002;23:1531–1536. [PubMed: 12116165]
9. Nakayama T, Kurosawa Y, Furui S, Kerman K, Kobayashi M, Rao SR, Yonezawa Y, Nakano K, Hino A, Yamamura S, Takamura Y, Tamiya E. Anal Bioanal Chem 2006;386:1327–1333. [PubMed: 16896609]
10. Nakano M, Komatsu J, Matsuura S, Takashima K, Katsura S, Mizuno A. J Biotechnol 2003;102:117–124. [PubMed: 12697388]
11. Margulies M, Egholm M, Altman WE, Attiya S, Bader JS, Bemben LA, Berka J, Braverman MS, Chen YJ, Chen Z, Dewell SB, Du L, Fierro JM, Gomes XV, Godwin BC, He W, Helgesen S, Ho CH, Irzyk GP, Jando SC, Alenquer ML, Jarvie TP, Jirage KB, Kim JB, Knight JR, Lanza JR, Leamon JH, Lefkowitz SM, Lei M, Li J, Lohman KL, Lu H, Makhijani VB, McDade KE, McKenna MP, Myers EW, Nickerson E, Nobile JR, Plant R, Puc BP, Ronan MT, Roth GT, Sarkis GJ, Simons JF, Simpson JW, Srinivasan M, Tartaro KR, Tomasz A, Vogt KA, Volkmer GA, Wang SH, Wang Y, Weiner MP, Yu P, Begley RF, Rothberg JM. Nature 2005;437:376–380. [PubMed: 16056220]
12. Williams R, Peisajovich SG, Miller OJ, Magdassi S, Tawfik DS, Griffiths AD. Nat Methods 2006;3:545–550. [PubMed: 16791213]
13. Diehl F, Li M, He Y, Kinzler KW, Vogelstein B, Dressman D. Nat Methods 2006;3:551–559. [PubMed: 16791214]
14. Leamon JH, Link DR, Egholm M, Rothberg JM. Nat Methods 2006;3:541–543. [PubMed: 16791212]
15. Thorsen T, Roberts RW, Arnold FH, Quake SR. Physical Review Letters 2001;86:4163–4166. [PubMed: 11328121]
16. Tan YC, Fisher JS, Lee AI, Cristini V, Lee AP. Lab on a Chip 2004;4:292–298. [PubMed: 15269794]
17. Garstecki P, Fuerstman MJ, Stone HA, Whitesides GM. Lab on a Chip 2006;6:437–446. [PubMed: 16511628]
18. Song H, Tice JD, Ismagilov RF. Angewandte Chemie-International Edition 2003;42:768–772.

19. Kumaresan P, Yang CJ, Cronier SA, Blazej RG, Mathies RA. Anal Chem 2008;80:3522–3529. [PubMed: 18410131]
20. Beer NR, Hindson BJ, Wheeler EK, Hall SB, Rose KA, Kennedy IM, Colston BW. Anal Chem 2007;79:8471–8475. [PubMed: 17929880]
21. Chabert M, Dorfman KD, de Cremoux P, Roeraade J, Viovy JL. Anal Chem 2006;78:7722–7728. [PubMed: 17105164]
22. Mohr S, Zhang YH, Macaskill A, Day PJR, Barber RW, Goddard NJ, Emerson DR, Fielden PR. Microfluidics and Nanofluidics 2007;3:611–621.
23. Whitesides GM, Ostuni E, Takayama S, Jiang X, Ingber DE. Annual Review of Biomedical Engineering 2001;3:335–373.
24. Fiorini GS, Chiu DT. Biotechniques 2005;38:429–446. [PubMed: 15786809]
25. Duffy DC, McDonald JC, Schueller OJA, Whitesides GM. Anal Chem 1998;70:4974–4984.
26. Gonzalez A, Grimes R, Walsh EJ, Dalton T, Davies M. Biomed Microdevices 2007;9:261–266. [PubMed: 17180709]
27. Anna SL. Applied Physics Letters 2003;82:364.
28. Reimann C, Filzmoser P, Garrett RG. Sci Total Environ 2005;346:1–16. [PubMed: 15993678]
29. Blodgett, R. Bacteriological Analytical Manual Online. Rockville, MD: Food and Drug Administration; 2001 [(accessed 21 March 2008)]. http://vm.cfsan.fda.gov/~ebam/bam-a2.html
30. Heid CA, Stevens J, Livak KJ, Williams PM. Genome Res 1996;6:986–994. [PubMed: 8908518]
31. Beer NR, Wheeler EK, Lee-Houghton L, Watkins N, Nasarabadi S, Hebert N, Leung P, Arnold DW, Bailey CG, Colston BW. Anal Chem 2008;80:1854–1858. [PubMed: 18278951]
32. Gersberg RM, Rose MA, Robles-Sikisaka R, Dhar AK. Appl Environ Microbiol 2006;72:7438–7444. [PubMed: 16980430]
33. Halvorson HO, Ziegler NR. J Bacteriol 1933;26:559–567. [PubMed: 16559678]
34. Link DR, Grasland-Mongrain E, Duri A, Sarrazin F, Cheng Z, Cristobal G, Marquez M, Weitz DA. Angew Chem Int Ed Engl 2006;45:2556–2560. [PubMed: 16544359]

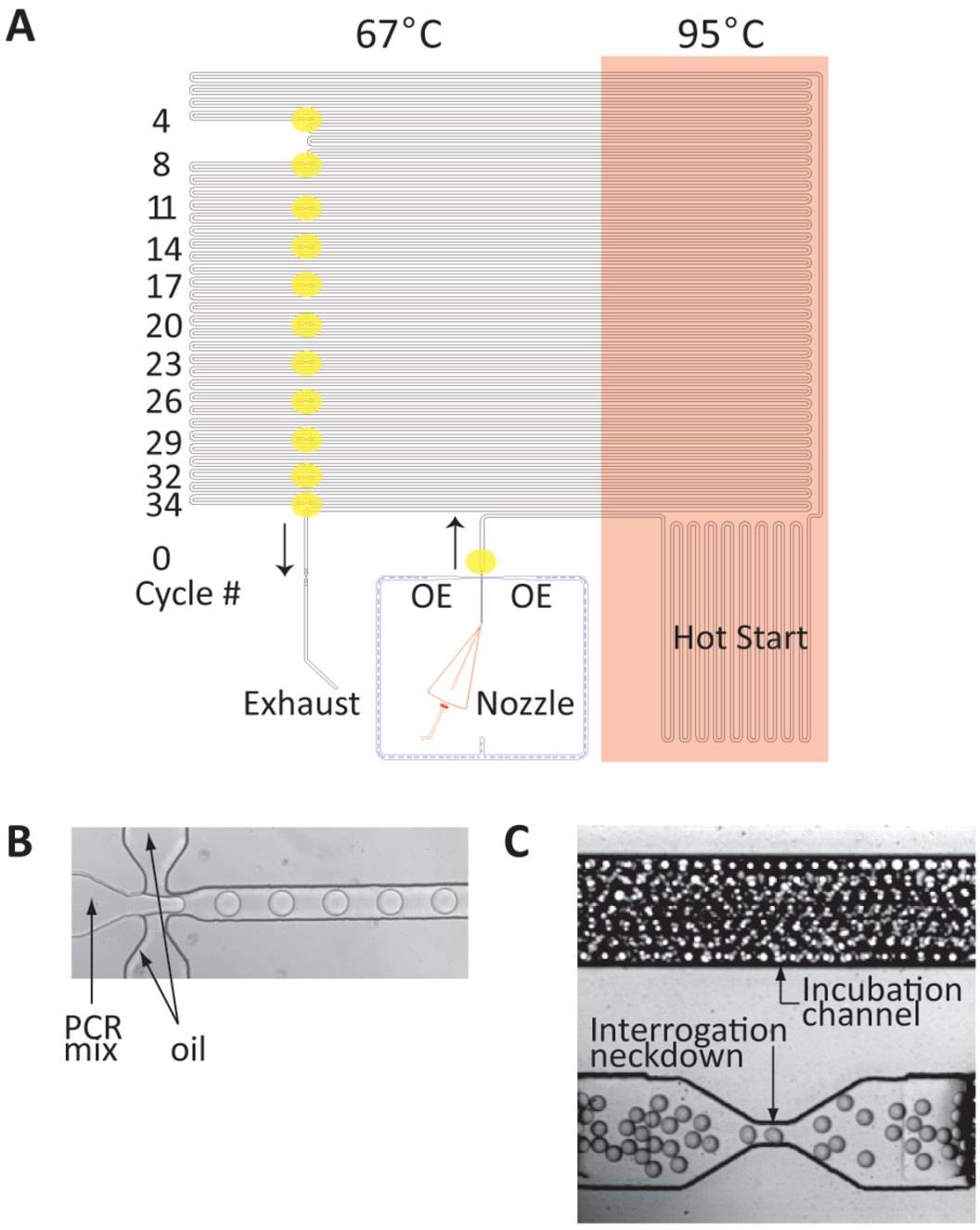

Figure 1.
Images of the PCR chip. (a) Schematic of the overall flow configuration. Pink-shaded regions of the chip were maintained at 95°C, and non-shaded regions were at 67°C. The regions highlighted in yellow correspond to the interrogation neckdowns, and the corresponding cycle numbers are noted on the left. The nozzle is highlighted in red, and the oil extractor (OE) is in blue. (b) Optical image of droplet generation at the nozzle. (c) Optical image of uniform droplets in the downstream channel and flowing through one of the neckdowns.

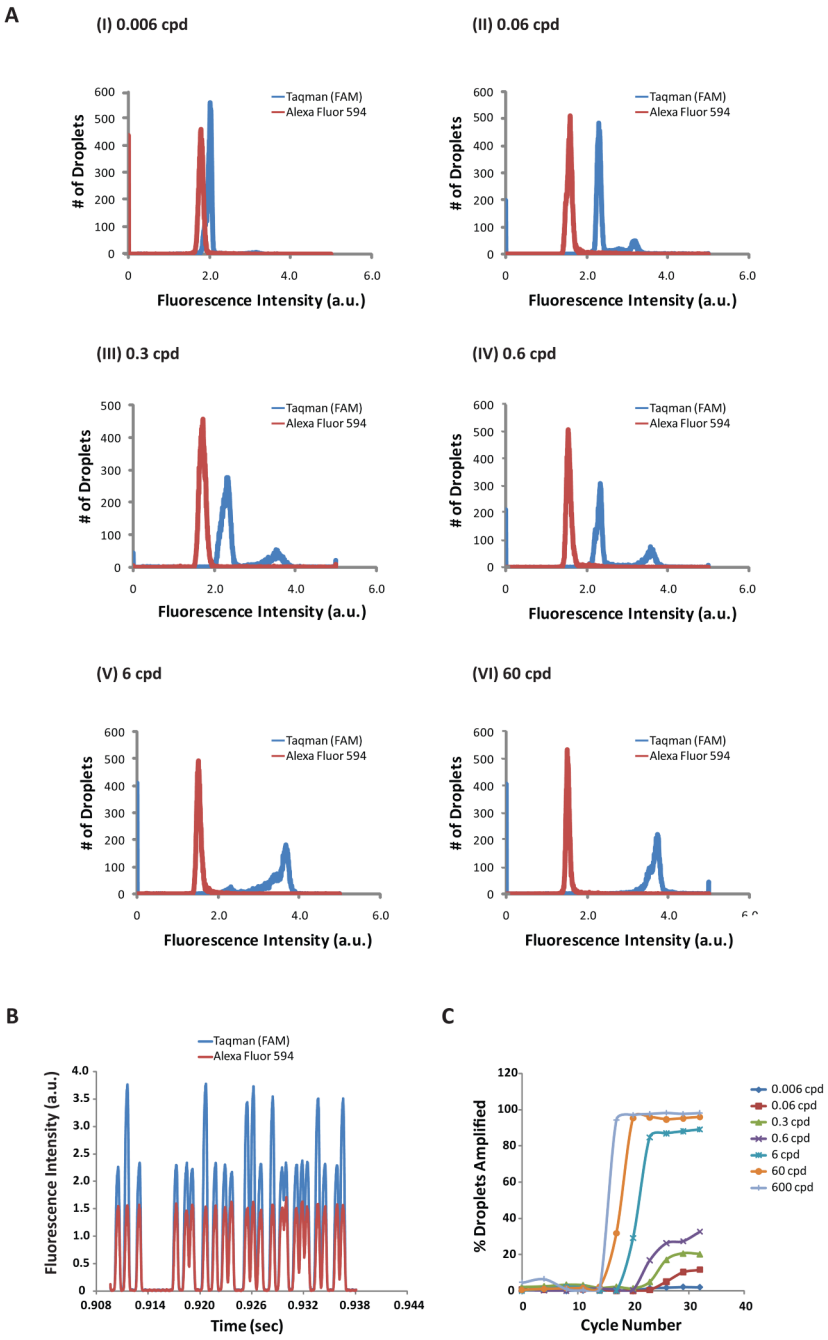

Figure 2.

Real-time PCR data from picoliter droplets. (a) Histogram showing the distribution of fluorescence signal (arbitrary units a.u.) among droplets passing through the excitation lasers (488 nm and 561 nm) at the interrogation neckdown on cycle 34. Histograms are shown for droplets containing an average of 0.006, 0.06, 0.3, 0.6, 6, and 60 copies of template DNA in panels I–VI, respectively. (b) Time trace (36 ms) of fluorescence signals (arbitrary units a.u.) from droplets passing one-by-one through the excitation lasers (488 nm and 561 nm) at the interrogation neckdown on cycle 34. The droplets on average are passing through the neckdown at 500 per second and contain an average of 0.6 copies of template DNA. (c) Time traces (30 s) were taken at every third cycle for each template concentration, and the percentage of

droplets with FAM fluorescence above the background level (PCR positive droplets) were plotted versus cycle number. Cpd = copies per droplet.

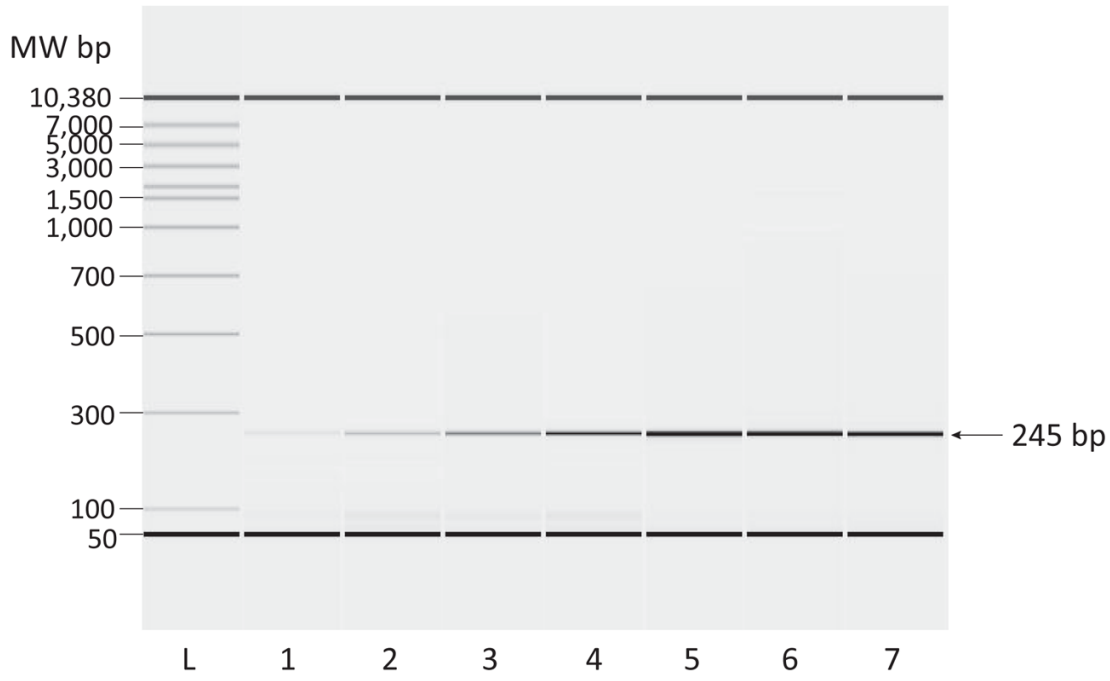

Figure 3.
Visual analysis of bulk PCR product for each template concentration by automated electrophoresis. Lanes 1 through 7 correspond to 0.006, 0.06, 0.3, 0.6, 6, 60, and 600 starting template copies per drop, respectively. Lane L represents the DNA ladder.

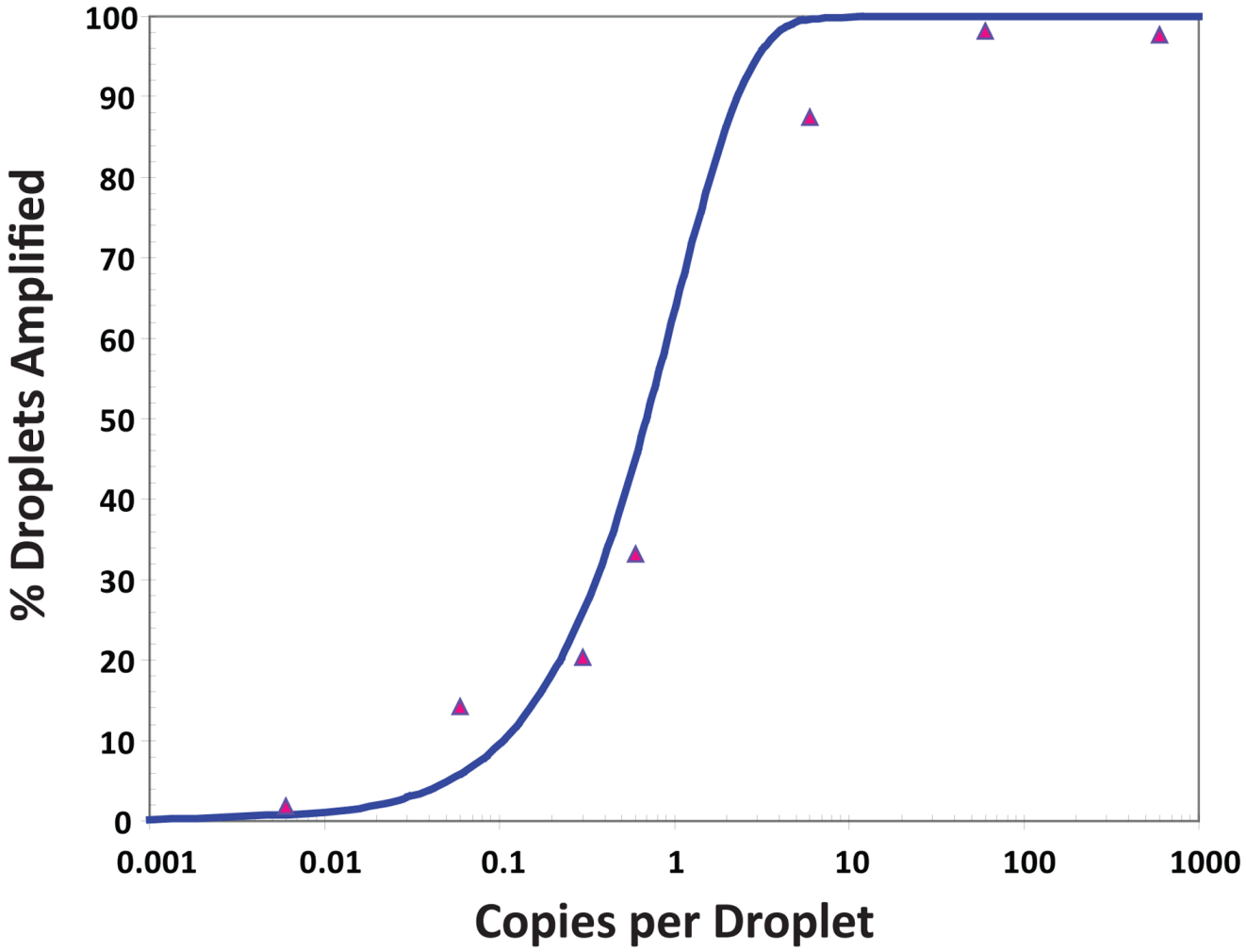

Figure 4.
Plot of the percentage of droplets that supported amplification versus starting copynumber. The curve represents the percentage expected from Poisson statistics (solid blue line).

Table 1

Sequences of primers and Taqman probe

Oligo	Sequence	Tm
Forward	5′-ACAAAGGCTCGCGTCCAGGC-3′	59.97
Reverse	5′-CAGCTGGCCCTCGCAGACAG-3′	59.77
Probe	5′FAM-ACATGTCGCCCTCTTCGGCATCA-3′B HQ1	68.9

Table 2

Picoliter droplet template concentrations and thresholds

Copies per droplet	Cycle Threshold (Ct)
600	16.1
60	17.9
6	21.2
0.6	n/a[a]
0.3	n/a[a]
0.06	n/a[a]
0.006	n/a[a]

[a] n/a, not applicable. For template concentrations of less than 1 copy per droplet, cycle thresholds could not be accurately computed from the average droplet fluorescence measurement, as the reactions contained a mixture of positive and empty droplets.

Table 3

Comparison of Observed Amplication Distribution to Poisson Statistics and MPN

Template Concentration		PCR Positive Droplets		
Copies per Droplet	**Copies per Droplet (MPN adjusted)** [a]	**Observed**	**Expected (Poisson)**	**Expected (Poisson, MPN adjusted)** [a]
0.006	0.0050 (± 0.000082)	2.08%	0.60%	0.49–0.51%
0.06	0.050 (± 0.00082)	11.7%	5.82%	4.76–4.95%
0.3	0.25 (± 0.0041)	20.3%	25.9%	21.6–22.4%
0.6	0.50 (± 0.0082)	32.6%	45.1%	38.6–39.8%
6	5.0 (± 0.082)	89.0%	99.8%	99.2–99.4%
60	50 (± 0.82)	95.9%	100%	100%
600	500 (± 8.2)	98.2%	100%	100%

[a] MPN calculation based on the 4 lowest dilutions was 0.83 ± 0.017. Adjusted values are within 95% confidence.